Available online at www.sciencedirect.com
ScienceDirect
International Journal of Multiphase Flow 32 (2006) 1017–1028
International Journal of Multiphase Flow
www.elsevier.com/locate/ijmulflow

Brief communication

Two phase liquid–liquid flows in pipes of small diameters

Adrian Wegmann, Philipp Rudolf von Rohr *

Institute of Process Engineering, Federal Institute of Technology, Sonneggstrasse 3, CH-8092 Zuerich, Switzerland

Received 24 January 2005; received in revised form 11 April 2006

Keywords: Two phase flow; Liquid–liquid; LIF; Flow map

1. Introduction

Continuous production in tubular reactors of small diameter is a promising topic for the pharmaceutical and the fine chemical industry. Small scaled tubular reactors provide some advantages in comparison to continuously stirred tank reactors. In the case of reactions with high hazard potential, small volumes result in a low impact of possible runaway reactions and in a favorable ratio of surface for heat exchange to volume. This fact allows a better control of the temperature inside the reactor and therefore an enhancement in the reaction control and higher yields. Reliable design of such facilities requires substantial knowledge of the flow inside the pipes. The knowledge of the flow pattern, that develops inside the pipe for special flow conditions is needed to estimate the area of contact between two immiscible fluids.

Charles et al. (1961) investigated equal density oil–water mixtures in a 1 inch pipe with oils of three different viscosities. Flow patterns, holdup ratios and pressure gradients were experimentally determined with the main interest in decreasing the pressure drop, which results from the introduction of water into pipelines during transportation of crude oil. Hasson et al. (1970) investigated the breakup of concentrically initialized flow of two immiscible liquids with a small density difference. Arirachakaran et al. (1989) investigated oil–water mixtures in 1 and 1.5 inch pipes. They varied the oil viscosities between 4.7 mPa s and 2116 mPa s. Correlations for the phase inversion point and the pressure drop of stratified and homogeneous flow patterns were developed. Beretta et al. (1997) investigated the oil–water flow patterns in a horizontal 3 mm inner diameter tube. They used three different oils with kinematic viscosities ranging from 9.8×10^{-4} m^2 s to 71.2×10^{-4} m^2 s. Nadler and Mewes (1997) investigated the effect of emulsification and phase inversion on the pressure drop for different flow regimes of two phase oil–water mixtures. They measured maximum pressure drops in the region of phase inversion, for input water fractions between 10% and 20%. Trallero et al. (1997) studied oil–water flow patterns in horizontal pipes. They divided the observed flow patterns in two groups, segregated and dispersed flows. Each group is further subdivided. Additionally the first complete model for predicting oil–water flow pattern transitions for light oils was proposed. Angeli and Hewitt (2000) investigated the flow structure in horizontal oil–water flows in a 24.3 mm pipe. They used both, a steel and an acrylic pipe to investigate the

* Corresponding author.
E-mail address: vonrohr@ipe.mavt.ethz.ch (Ph. Rudolf von Rohr).

doi:10.1016/j.ijmultiphaseflow.2006.04.001

influence of the wetting parameters of the fluids to different wall materials. Simmons and Azzopardi (2001) measured drop size distributions for oil–water systems in a 63 mm pipe. They compared their results to the flow map proposed by Trallero et al. (1997). Liu et al. (2003) investigated flow patterns and their transitions of oil–water systems in a 40 mm inner diameter pipe. In a similar way to Angeli and Hewitt (2000) they used both a stainless steel and a plexi-glas pipe. Additionally, they developed semi theoretical transition criteria to predict the transition lines. Bannwart et al. (2004) studied the flow patterns formed by heavy crude oil and water inside vertical and horizontal 28.4 mm pipes. Sotgia and Tartarini (2004) gave an overview on the state of the art and recent developments on pressure drop reductions and flow regimes of oil–water flows in horizontal pipes. Also, Yang et al. (2004) investigated the approach to stratification of a dispersed liquid–liquid flow at a sudden expansion. The flow patterns they observed were compared with the one proposed by Trallero et al. (1997).

2. Experimental setup

The experiments are carried out in the multiphase flow facility shown in Fig. 1. Water and paraffin-oil are stored in 70 l tanks. The pipe is made of glass (Schott Duran®) and has a total length, between the entrance section and the separation container, of 5 m. The pipeline consists of five sections, each with a length of 1 m. Pressure is measured with Endress–Hauser® pressure transducers type Cerabar T PMC 131 with a shelf accuracy of 0.02 bars. Temperature is measured with Thermocoax® Thermocouples with a shelf accuracy of 0.1 °C. Pictures of the flow are taken with a high resolution digital camera (Minolta Dimage 7i with a resolution of 2560×1920 pixels). With a view area of 48 mm × 36 mm. This results in a resolution of 0.019 mm per pixel. The camera used has a relatively low shutter-speed of 1/2000 s in minimum. To minimize the displacement of the flow during the time when the shutter is open, the product of the lighting time, times the velocity, has to be smaller than the resolution of the pictures (0.019 mm). With a maximum speed of the mixture ($U_{\text{Mixture}} = 4.5$ m/s) this results in a lighting time smaller than 4.2 μs. To achieve this, two devices are being used. A strobo-scope (Strobotac® 1538-A) with a flash duration between 0.5 μs and 3.5 μs is used as source for transmitting light. This method is similar to the one used by Ward and Knudsen (1967). Also a laser sheet generated by an Argon–Ion laser (Coherent® Innova 305) and pulsed by a chopper wheel (HMS Lightbeam Chopper 221) is used. The laser light excites the uranine in the water phase (see below). This illumination

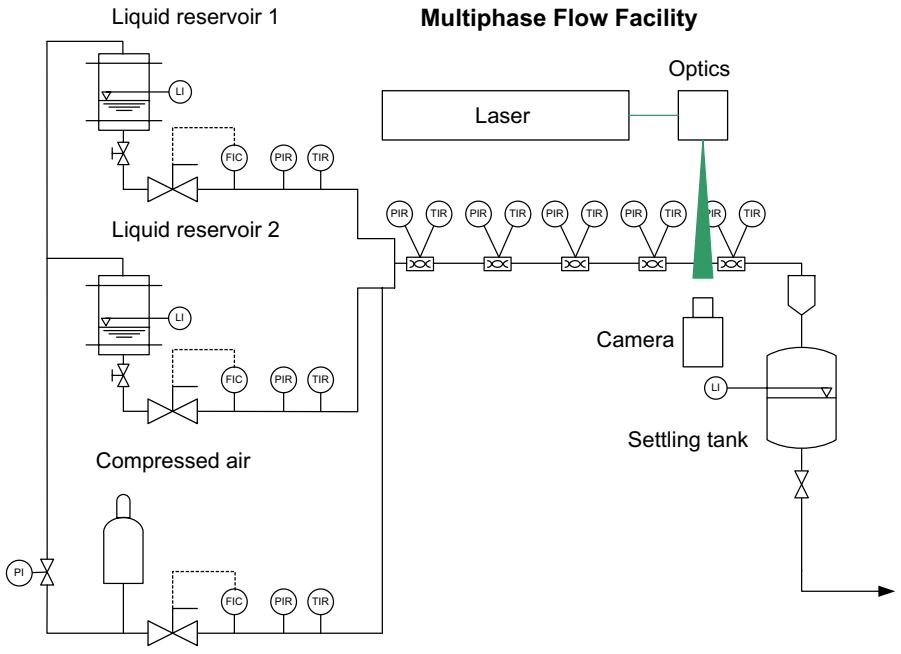

Fig. 1. Schematic diagram of the experimental setup.

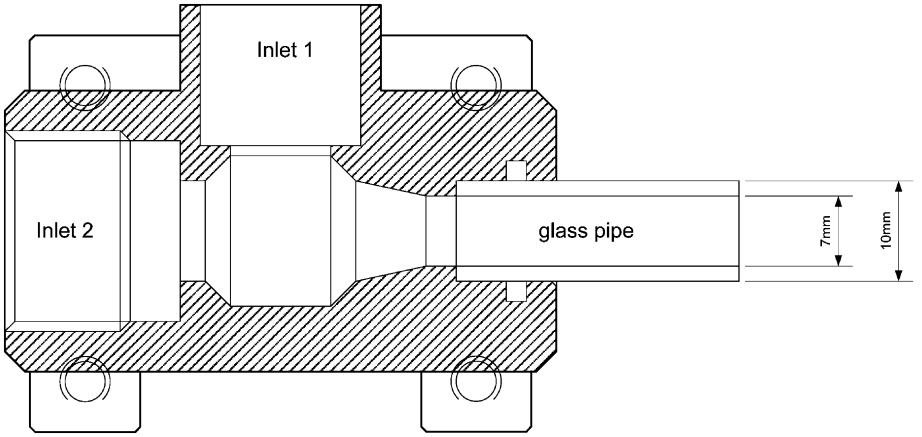

Fig. 2. T-shaped connecting piece.

technique gives very good contrast between the two phases because the oil will not emit any light. Pictures taken from the system illuminated by the laser provide information about the flow structure in a cross section of the pipe. This allows to analyze flow patterns with higher dispersities. Pictures of the flow are taken at a distance of 3.7 m from the entrance of the pipe. This corresponds to 660 pipe diameters for the 5.6 mm pipe and 528 pipe diameters for the 7 mm pipe. At this position the flow can be considered fully developed and any influences of the inlet configuration are negligible.

As the water phase, deionised water, dyed with uranine (fluorescein sodium salt) is used. The surface tension of the water phase is $\sigma_{\text{Water}} = 78.7 \times 10^{-3}$ N/m (at 20 °C). As the oil phase, low viscosity paraffin is used with a surface tension of $\sigma_{\text{Paraffin}} = 29.6 \times 10^{-3}$ N/m (at 20 °C). The interfacial tension between the two fluids is $\sigma_{\text{Paraffin}} = 62.2 \times 10^{-3}$ N/m (at 20 °C). Surface tensions are measured with a "Kruess G 10" contact angle measurement device. The storage tanks are pressurized with compressed air up to 6 bars. The mass flow rates of the liquids are controlled by two coriolis type mass flow controllers with a maximum mass flow rate of 180 kg/h and an accuracy of 0.2% of the desired flow rate. In the experiments the water and paraffin superficial velocities are varied in the range from $U_{\text{Water}} = 0.01$ m/s to $U_{\text{Water}} = 2.0$ m/s and $U_{\text{Paraffin}} = 0.01$ m/s to $U_{\text{Paraffin}} = 2.5$ m/s for the 5.6 mm pipe and from 0.01 m/s to 1.3 m/s and 0.01 m/s to 1.6 m/s for the 7 mm pipe, respectively. Due to temperature changes in the experimental facility between $T = 19.1$ °C and $T = 23.3$ °C, density and viscosity of the fluids vary. The water and paraffin densities varied in the range from $\rho_{\text{Water}} = 997.4$ kg/m^3 to $\rho_{\text{Water}} = 998.3$ kg/m^3 and $\rho_{\text{Paraffin}} = 818.0$ kg/m^3 to $\rho_{\text{Paraffin}} = 820.5$ kg/m^3, respectively. The water and paraffin viscosities varied in the range from $\eta_{\text{Water}} = 0.7$ mPa s to $\eta_{\text{Water}} = 0.9$ mPa s and $\eta_{\text{Paraffin}} = 4.3$ mPa s to $\eta_{\text{Paraffin}} = 5.2$ mPa s respectively. The water density and viscosity is calculated according to the international standard IAPWS-IF97 (Wagner and Kruse, 1998). The paraffin density and viscosity are calculated according to Stahl (2002). The pure phases of paraffin and water are fed into the pipe by a T-shaped connecting piece as shown in Fig. 2. This design has been selected to prevent the formation of emulsions due to mixing effects taking place in the entrance area. In this study only the effects of the pipe flow are investigated.

3. Results

Concerning the number of distinguishable flow pattern, one can find different opinions in literature. Depending on the variety of flow conditions obtained during the experiments, the number of observed flow patterns can be up to 16, as defined by Wong and Yau (1997). In this work the main flow regimes that have been observed in horizontal liquid–liquid flows are described according to Barnea et al. (1983).

Due to the comparability to other flow maps, only the four main flow patterns are used in this work. In the flow pattern maps the data are presented as the mixture velocity U_{Mixture} vs. the input water volume fraction $\dot{\varepsilon}_{\text{Water}}$. In the following, the observed flow patterns are presented in the order of increasing mixture velocity

U_{Mixture} (see Eq. (1)) where $\dot{V}_{\text{Water}}$ is the volume flow rate of the water, $\dot{V}_{\text{Paraffin}}$ is the volume flow rate of the paraffin and A_{Pipe} is the cross sectional area of the pipe. The borders between the different flow regimes are plotted as sharp lines but in reality these transitions progress smoothly. Hysteresis effects are not observed

$$U_{\text{Mixture}} = \frac{\dot{V}_{\text{Water}} + \dot{V}_{\text{Paraffin}}}{A_{\text{Pipe}}} \tag{1}$$

$$\dot{\varepsilon}_{\text{Water}} = \frac{\dot{V}_{\text{Water}}}{\dot{V}_{\text{Water}} + \dot{V}_{\text{Paraffin}}} \tag{2}$$

For the sake of comparability, mixture Reynolds numbers Re_{Mixture} are always composed with the viscosity of the water phase η_{Water}

$$Re_{\text{Mixture}} = \frac{U_{\text{Mixture}} \times D_{\text{Pipe}} \times \rho_{\text{Mixture}}}{\eta_{\text{Water}}} \tag{3}$$

$$\rho_{\text{Mixture}} = \rho_{\text{Water}} \times \dot{\varepsilon}_{\text{Water}} + \rho_{\text{Paraffin}} \times (1 - \dot{\varepsilon}_{\text{Water}}) \tag{4}$$

The density of the mixture ρ_{Mixture} is calculated with the input water volume fraction, provided that the slip velocity ratio s satisfies Eq. (5) along the whole pipe

$$s = \frac{U_{\text{Water}}}{U_{\text{Paraffin}}} \approx 1 \tag{5}$$

Identification of the flow patterns was done by visual observation of the flow during the experiments and evaluation of the pictures. Intrusive measurement methods were not applied to avoid flow disturbances.

3.1. Stratified flow

The two fluids flow in separate layers according to their densities. Stratified flow occurs for input water volume fraction $\dot{\varepsilon}_{\text{Water}} < 0.5$ and mixture velocities $U_{\text{Mixture}} < 1.9$ m/s. Fig. 3 shows a typical example for a stratified flow. With lower paraffin volume fractions and higher velocity, stratified wavy flows develop. This means, that due to the Kelvin–Helmholtz effect waves are generated on the water paraffin interface, but the properties of the flow do not allow the waves to grow and stratification is not destroyed.

3.2. Intermittent flow

This flow pattern is specified by: no stratification of the two phases, no continuous core inside an annulus and no uniform dispersion of one phase inside the other. Barnea et al. (1983) divided intermittent flows into elongated bubble flow and slug flow. Fig. 4 shows an intermittent flow, for a water volume fraction of $\dot{\varepsilon}_{\text{Water}} < 0.291$ and mixture velocities $U_{\text{Mixture}} < 0.86$ m/s. Large continuous oil pockets, almost filling the pipe cross section, are transported within the flow.

Fig. 3. Stratified flow pattern in the 5.6 mm pipe. Mixture velocity $U_{\text{Mixture}} = 0.70$ m/s, input water volume fraction $\dot{\varepsilon}_{\text{Water}} = 0.291$, Reynolds number of the mixture $Re_{\text{Mixture}} = 3'410$.

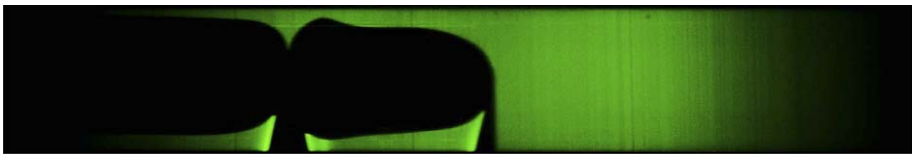

Fig. 4. Intermittent flow pattern in the 5.6 mm pipe. Mixture velocity $U_{\text{Mixture}} = 0.86$ m/s, input water volume fraction $\dot{\varepsilon}_{\text{Water}} = 0.711$, Reynolds number of the mixture $Re_{\text{Mixture}} = 4'547$.

3.3. Annular dispersed flow

Analyzing annular flows in literature, it shows up, that always the fluid with the smaller density is building the core flow (Barnea et al., 1983; Hasson et al., 1970; Sotgia and Tartarini, 2004). As already mentioned in stratified flows, with increasing slip velocity waves appear on the interface of the fluids and also drops or bubbles can rip of the waves and get dispersed in the other fluid. In this work, for higher mixture velocities and water fractions between 0.1 and 0.5, the annular dispersed flow, shown in Fig. 5 develops.

3.4. Dispersed flow

For low volume fractions of one phase and high mixture velocities, the dispersed phase is distributed in small droplets. In most cases, water is the continuous phase, that means water is wetting the whole pipe wall. Phase inversion, where paraffin is wetting the whole circumference of the pipe, only takes place at paraffin volume fractions $\dot{\varepsilon}_{\text{Paraffin}} > 0.8$ and high Reynolds numbers. The droplet size, which depends on the turbulence, decreases with increasing velocity. With paraffin as the continuous phase, dispersed flows develop for much lower velocities than using water as the continuous phase. This is due to the difference in viscosity between the two fluids. When water wets the pipe wall, the thickness of the laminar sublayer is smaller because of the smaller viscosity. Thus, the pressure drop will be smaller than if paraffin was the outer phase (see Fig. 6). The thickness of the laminar sublayer δ_l is calculated by Eq. (6), as proposed by Prandtl:

$$\delta_l = D_{\text{Pipe}} \frac{62.7}{Re_{\text{Mixture}}^{7/8}} \tag{6}$$

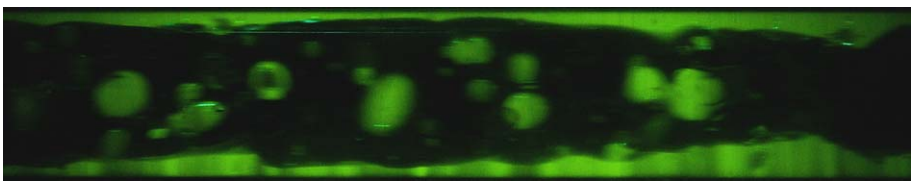

Fig. 5. Annular dispersed flow pattern in the 5.6 mm pipe. Mixture velocity $U_{\text{Mixture}} = 2.10$ m/s, input water volume fraction $\dot{\varepsilon}_{\text{Water}} = 0.291$, Reynolds number of the mixture $Re_{\text{Mixture}} = 10'231$.

Fig. 6. Dispersed flow pattern in the 5.6 mm pipe. Mixture velocity $U_{\text{Mixture}} = 1.94$ m/s, input water volume fraction $\dot{\varepsilon}_{\text{Water}} = 0.105$, Reynolds number of the mixture $Re_{\text{Mixture}} = 9'095$.

The values of δ_l for turbulent flows, which means $Re_{\text{Mixture}} > 2000$ range from 0.076 mm and 0.3 mm in the 7 mm pipe and from 0.051 mm to 0.34 mm in the 5.6 mm pipe.

3.5. Mechanisms leading to flow-pattern transition

All the flow conditions, used in this study, show within the first part of the pipe stratified flow condition. The specific flow patterns develop during the flow along the pipe. The mechanisms that lead from one pattern to another are explained below. Fig. 7 shows the experimental transition lines from the 5.6 mm pipe.

3.5.1. Stratified → dispersed paraffin continuous

Transition I, in Fig. 7, represents the experimental boundary between stratified flow and the dispersed flow where paraffin is the continuous phase. In this range of the input water volume fraction, the water film at the bottom of the pipe is rather thin. When the mixture velocity reaches the value of about 2 m/s, the turbulent energy is high enough to break up all the water in small droplets which are dispersed in the continuous paraffin.

3.5.2. Stratified → annular dispersed

Along transition II in Fig. 7, enough water is available to build up an annulus. The water is swept up along the pipe wall until it wets the whole circumference of the pipe. An annular flow, where paraffin is the wall-wetting phase was never found. Taking into account the results of other authors (Baker, 1954; Charles et al., 1961; Hasson et al., 1970; Mandhane et al., 1974), it can be assumed, that in annular flow the phase with the smaller density is building the core flow.

3.5.3. Stratified → intermittent

For transition III, on the interface between water and paraffin, waves are generated, caused by the Kelvin–Helmholtz instabilities. Some of these waves increase until they reach the top of the pipe. In this way, sections

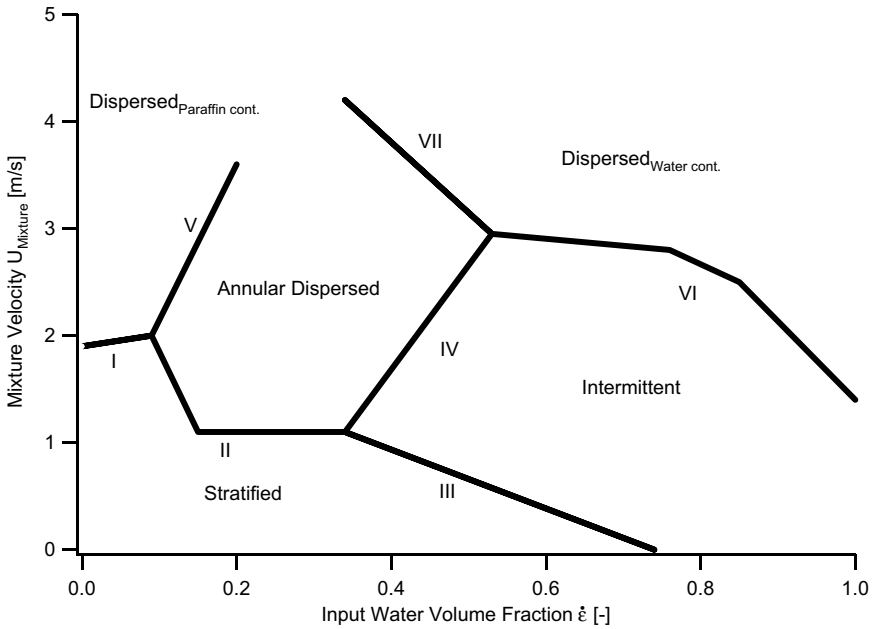

Fig. 7. Boundaries between flow patterns from the experiments in the 5.6 mm pipe: numbered for the purpose of theoretical considerations.

develop where water is filling up the whole cross section. The length of these sections depends on the water fraction inside the pipe.

3.5.4. Annular dispersed → intermittent

The breakup of an annular flow structure to intermittent structures, transition IV on Fig. 7, occurs due to two different mechanisms. Hasson et al. (1970) describe these two mechanisms as follows:

- Top wall film rupture. For low water fractions, and accordingly low mixture velocities, the core ascent due to buoyancy to the top wall of the pipe and brakes through the annular film. Segments of water are generated, filling up the whole cross section of the pipe. This is due to the velocity, which is too high to allow stratified flow to develop.
- Collapse of the core due to interfacial waves. For higher water fractions and accordingly higher mixture velocities, the waves on the interface between water and paraffin grow and get connected. In this way an intermittent flow develops.

3.5.5. Dispersed paraffin continuous → annular dispersed

At the crossing transition line V, in the dispersed flow pattern, the turbulent energy is high enough to maintain the water droplets dispersed in the paraffin core. With increasing water fraction, the droplets get bigger and decline to the bottom of the pipe. Here, the droplets coalesce and build a layer. Due to the high mixture velocity an annular flow is generated according to Section 3.5.

3.5.6. Intermittent → dispersed water continuous

In transition VI the turbulent energy is high enough to break up all the paraffin into small droplets. Accordingly, the mixture velocity necessary to get the paraffin dispersed decreases with decreasing paraffin volume fraction.

3.5.7. Annular dispersed → dispersed water continuous

The paraffin core collapses into droplets due to turbulences. The necessary mixture velocity decreases with decreasing paraffin volume fraction. This describes transition line VII.

3.6. Flow map

The literature review showed that there is no generalized flow pattern map for the horizontal flow of two immiscible liquids. A survey of literature data on flow maps for liquid–liquid systems follows. Nadler and Mewes (1997) use two graphic renditions: superficial velocities of the two phases and the velocity of the mixture vs. the input water fraction. The latter way of presenting the data is also used by Angeli and Hewitt (2000). Hasson et al. (1970) presented their data in diagrams with axes denoting the volume flow rates of the two liquids. Baker (1954) used G/λ vs. $L\lambda\psi/G$ and Hapanowicz and Troniewski (2002) used the superficial velocity of the water vs. the ratio of the superficial velocities. This variety exists because it is not possible to show all the influences in a two dimensional diagram.

Figs. 8 and 9 show the flow maps generated from the results of the experiments using a 7 mm and a 5.6 mm pipe respectively. The y-axis denotes the velocity of the liquid mixture U_{Mixture} (Eq. (1)) and the x-axis denotes the input water fraction $\dot{\varepsilon}_{\text{Water}}$ (Eq. (2)). This graphic rendition was chosen because it visualizes the influence of the pipe diameter. These flow maps are based on 314 experiments.

Fig. 10 shows a direct comparison between the transition lines of the 5.6 mm and the 7.0 mm pipe. Some obvious differences between these transition lines are as follows:

- In the small pipe, dispersed flows show up for higher mixture velocities. This is due to the degree of turbulence, which is higher in the bigger pipes (see Eq. (3)).
- The areas where annular and intermittent flow structures exist, are in the small pipe considerably larger than in the 7.0 mm pipe. This is because a smaller pipe diameter discriminates stratified flows and dispersed flows as it is described above.

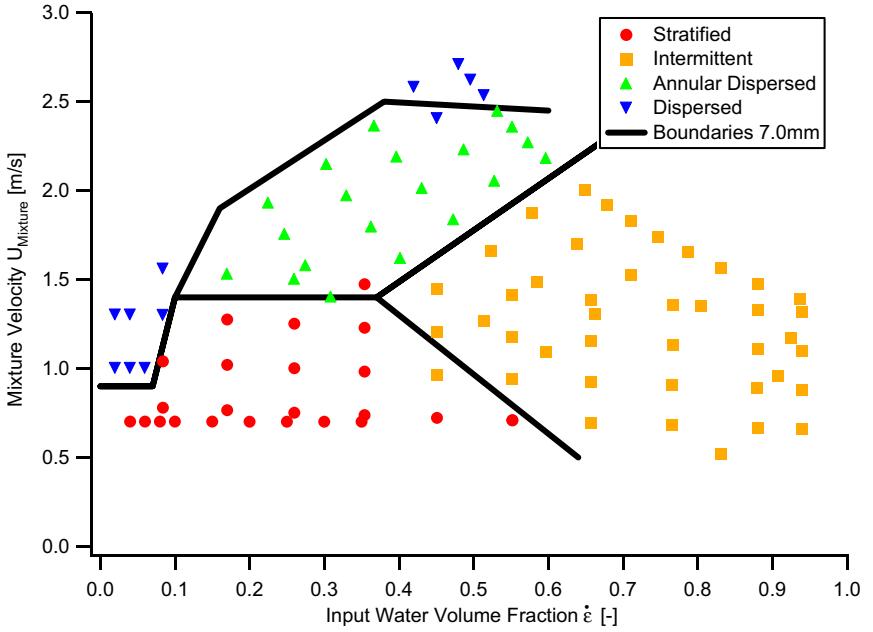

Fig. 8. Flow map for liquid–liquid flows in the 7 mm inner diameter glass pipe according to Angeli and Hewitt (2000). The indicated boundaries have no theoretical background, they are simply drawn between the regions of the different flow structures.

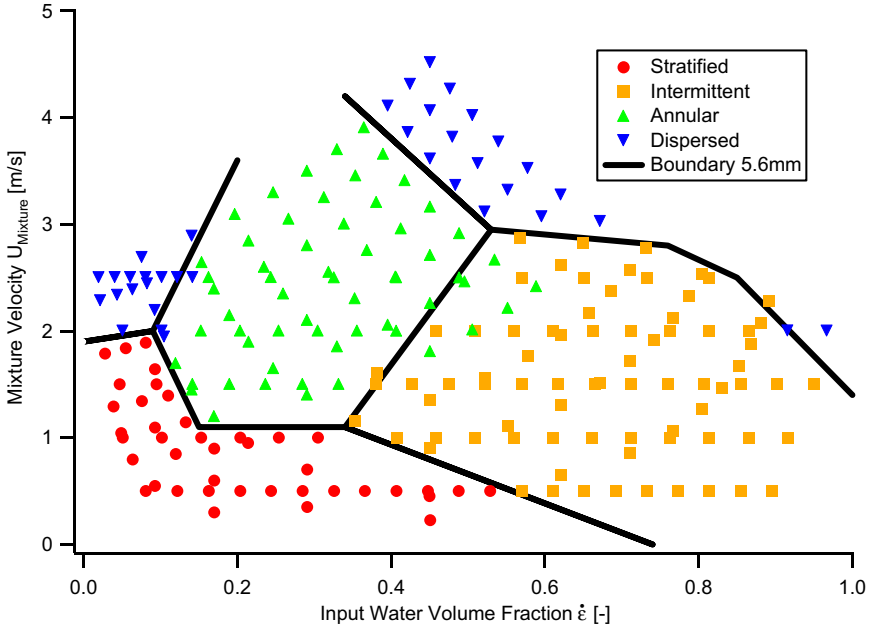

Fig. 9. Flow map for liquid–liquid flows in the 5.6 mm inner diameter glass pipe according to Angeli and Hewitt (2000). The indicated boundaries have no theoretical background, they are simply drawn between the regions of the different flow structures.

- The transition from stratified flow to other flow structures shows up for lower velocities in the 5.6 mm pipe. This is assumed to be due to the increasing impact of the surface tension forces compared to the buoyancy forces with decreasing diameter.

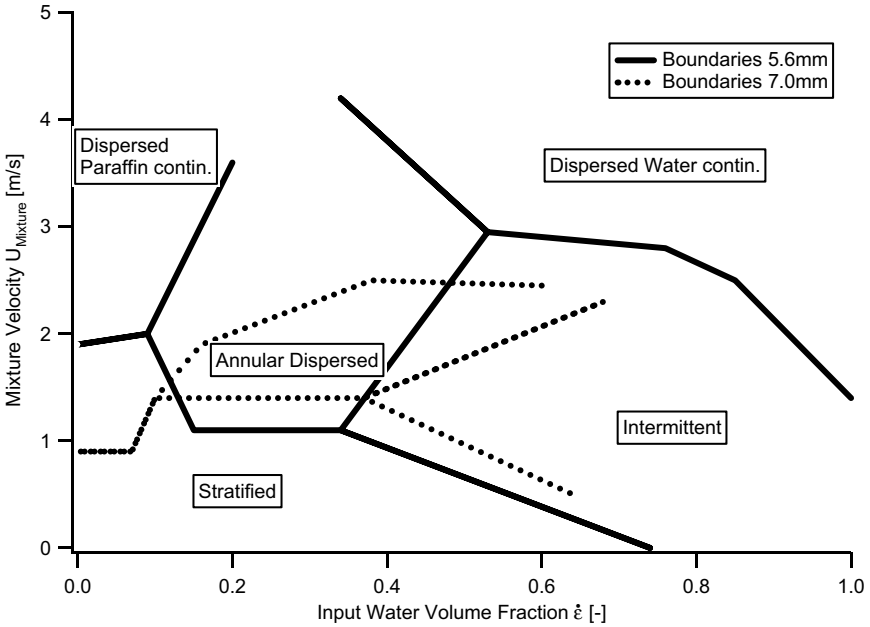

Fig. 10. Direct comparison of the boundaries of the 5.6 mm and the 7.0 mm pipe employed.

This last assumption is supported by an analysis with respect to the Bond number

$$Bo = \frac{(\rho_{\text{Water}} - \rho_{\text{Paraffin}}) \times g \times D_{\text{Pipe}}^2}{\sigma} \tag{7}$$

which means, for $Bo > 1$ gravitational forces are dominant and for $Bo < 1$ surface tension forces are dominant. In this work, for the 5.6 mm pipe, the Bond number is $Bo = 0.891$ and for the 7.0 mm pipe it is $Bo = 1.393$. So in the small pipe, surface tension is stronger than in the bigger pipe. This finding is supported by the observations.

The experiments carried out in this study have been compared to the flow maps proposed by Angeli and Hewitt (2000) and Hasson et al. (1970). The main properties of the investigated fluids and pipe diameters are displayed in Table 1.

The work of Angeli and Hewitt (2000) shows three main differences compared to this study. Firstly, the interfacial tension between the two phases is lower by a factor of 3.6. Secondly, the viscosity of the organic phase is lower by a factor of 3.1 and thirdly, the pipe diameter is larger by a factor of 3.74 or 4.33 in comparison to the 7 mm and the 5.6 mm pipe. This leads to considerable changes in the flow map as can be seen in Fig. 11 and are further discussed below. The flow patterns named in Fig. 11 are according to Angeli and Hewitt (2000).

Table 1
Major properties of experiment facilities

	Angeli	Hasson	Nadler	This work
$\frac{\rho_{\text{Water}}}{\rho_{\text{Paraffin}}}$ [–]	1.25	0.98	1.17	1.22
$\sigma_i[\frac{\text{N}}{\text{m}}]$	17×10^{-3}	17.5×10^{-3}	–	62×10^{-3}
$\frac{\eta_{\text{Water}}}{\eta_{\text{Paraffin}}}$ [–]	~0.6	~0.8	~0.03	~0.2
D_{Pipe} [m]	24.3×10^{-3}	12.6×10^{-3}	59×10^{-3}	7×10^{-3}; 5.6×10^{-3}
T [°C]	20	30	18–30	19–22

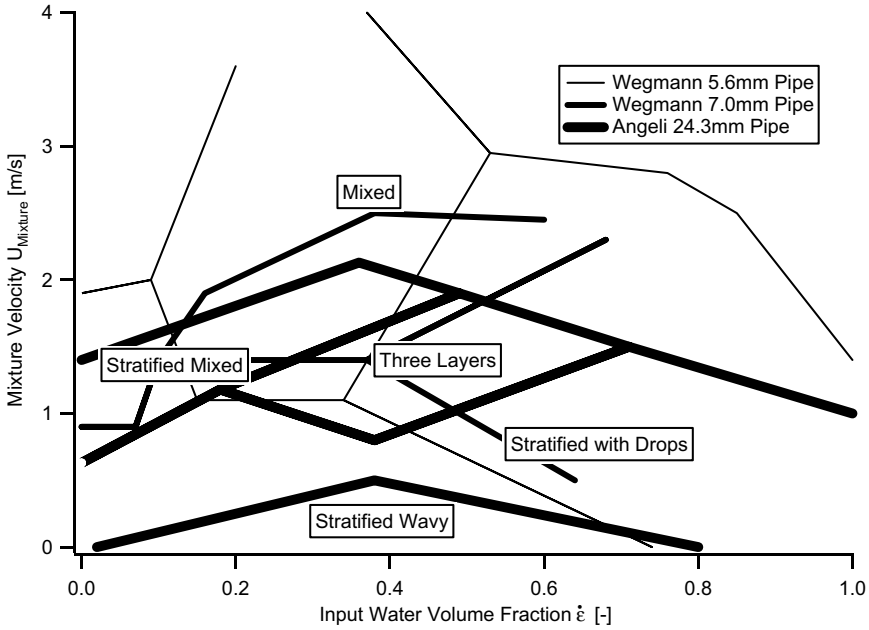

Fig. 11. Experimental transition lines of the present work compared to Angeli and Hewitt (2000).

The largest difference is that Angeli and Hewitt (2000) did not observe any intermittent flow. Most of their data points stand for different kinds of stratified flow. The region where stratified flow occurs is much larger than in the present study, where, above an input water fraction of 0.4 the interfacial tension forces overcome gravitational forces and water becomes the continuous phase. Intermittent flow develops. Because of the smaller interfacial tension, Angeli and Hewitt (2000) did not reach conditions where intermittent flow can exist. The mixed flow pattern is described as one phase assuming uniform dispersion, making no difference between paraffin or water as the continuous phase. Hence, Angeli and Hewitt (2000) found that for mixture velocities higher than 2 m/s always fully dispersed flow takes place. In the present study this happens for mixture velocities higher than 2.5 m/s in the 7.0 mm pipe and higher than 3.0 m/s in the 5.6 mm pipe. This is due to the higher surface tension existing between the fluids used in this study which prevents the dispersed phase from building small droplets. Also, the smaller pipe diameter in this study contributes to this effect because of the Reynolds number, which increases with increasing the pipe diameter.

Fig. 12 shows the comparison of the experimental data with the flow map of Hasson et al. (1970). Hasson et al. (1970) found that the oil along the pipe wall flowed in an annular flow while in the present study, in annular flow, always water was the outer phase. This is the reason why in Fig. 12 the axes are interchanged with respect to water and paraffin. Another major difference between Hasson et al. (1970) and the present work is the density ratio and the viscosity ratio of the two fluids. As noted in Table 1 the oil density in Hasson et al. (1970) is higher than the water density and the viscosities of the two fluids are similar. In comparison to the present study, the interfacial tension is 3.5 times lower in Hasson et al. (1970). The pipe diameter is 12.7 mm. Fig. 12 shows a direct comparison of the experimental transition lines of the present study compared to the results obtained by Hasson et al. (1970).

Starting the comparison from the area where stratified flow occurs, it can be seen, that for both, the 5.6 mm and the 7 mm pipe, stratified flow occurs for the same range of the paraffin flow rate. The range where stratified flow occurs in the 7 mm pipe contains the stratified area of the Hasson experiments. The special shape of the stratified area found by Hasson may be caused by the very small density difference. This leads to a less stable situation in stratified flows. Hasson et al. (1970) found simple annular flow which develops from elongated slugs that coalesce during flow along the pipe. Here, one has to take into account that Hasson et al. (1970) explicitly wanted to study the behavior of annular two phase flow in pipelines. In the present study the simple annular flow does not exist at all. When the paraffin volume fraction is high enough so that the

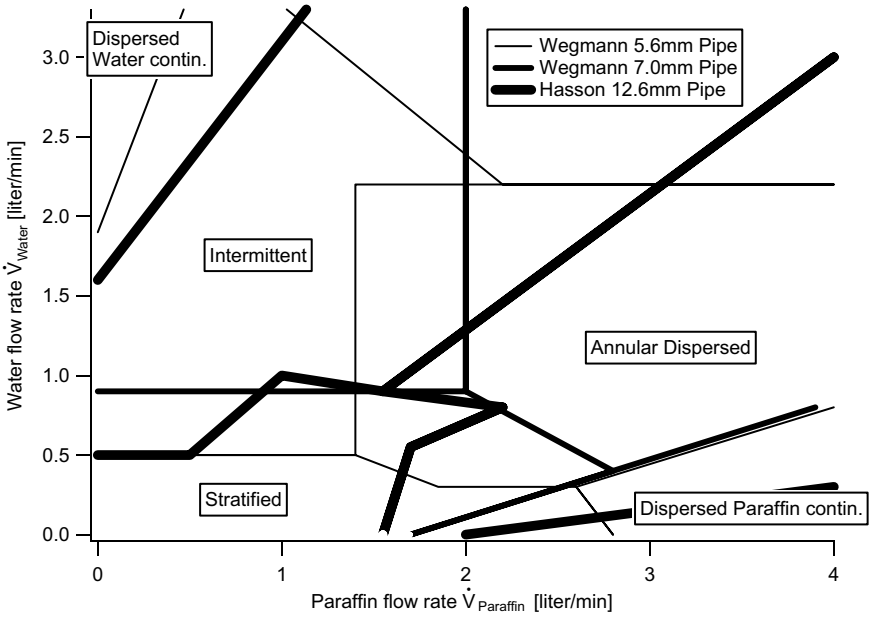

Fig. 12. Experimental transition lines of the present work compared to those found by Hasson et al. (1970).

plugs can coalesce to a core, there are many droplets which are small enough to persist in the annular water layer and also many water droplets inside the paraffin core. The greatest area in the flow map of Hasson et al. (1970) is the one with elongated slugs (see Fig. 12) which is comparable to the intermittent flow in the present study. The annular mixed flows of the present study, which are in the region of elongated slugs of Hasson et al. (1970) exist because of the higher viscosity of the organic phase and the higher surface tension. The annular flow reduces the surface energy because of the smaller specific surface area of the cylindrically shaped core flow. Concerning dispersed flows, Hasson et al. found dispersed flows only for either high paraffin volume fractions or high water volume fractions. The results for the 5.6 mm pipe show, that intermittent and annular dispersed flow is enveloped by dispersed flow on the upper right side if only the mixture velocity U_{Mixture} is high enough.

4. Conclusions

For the investigated pipes with a diameter of 5.6 mm and 7 mm, three major differences to the flow maps observed in larger pipes were found: first, stratified flows occur in a much smaller area of flow properties than in bigger pipes. This is due to the interaction of interfacial tension forces and gravitational forces. The smaller the pipe diameter is, the easier interfacial tension forces can overcome gravitational forces and the phase with the lower viscosity can wet the whole circumference of the pipe and plug flow can develop. Second, dispersed flows occur with higher velocities than in bigger pipes. The specific surface area is related to the degree of turbulence, which is quantified by the Reynolds number (see Eq. (3)). The higher the degree of turbulence is, and as well the Reynolds number, the higher the specific surface will be. And because the Reynolds number decreases with decreasing pipe diameter, in smaller pipes a higher velocity is needed to maintain the turbulence. Third, the area where intermittent flows occur grows with decreasing pipe diameter. This is because with decreasing pipe diameter, stratified flows are discriminated by the increasing influence of surface tension forces and dispersed flows are discriminated by the decreasing turbulence.

In the following the most important properties are listed and their effects on the flow patterns are described.

4.1. Density ratio

$$\hat{\rho}_{\text{Fluid}} = \frac{\rho_{\text{Water}}}{\rho_{\text{Organic}}} \tag{8}$$

Which phase is the upper one in stratified flows is the responsibility of the ratio between the densities of water and the organic fluid. The more this ratio is apart from unity, the easier stratified flows can develop.

4.2. Viscosity ratio

$$\hat{\eta}_{\text{Fuild}} = \frac{\eta_{\text{Water}}}{\eta_{\text{Organic}}} \tag{9}$$

The more the ratio between the viscosities of water and the organic phase differs from unity, the easier annular flows develop. This reduces the pressure drop because of the thinner laminar sub layer. This effect becomes more important the higher the Reynolds number is.

4.3. Interfacial tension σ_i

The interfacial tension between the two fluids has an influence on the transitions between the flow patterns. The lower the interfacial tension is, the easier the specific surface area can be increased. This means, for systems with lower interfacial tensions, dispersions are achieved for lower Reynolds numbers.

References

Angeli, P., Hewitt, G.F., 2000. Flow structure in horizontal oil–water flow. Int. J. Multiphase Flow 26, 1117–1140.

Arirachakaran, S., Oglesby, K., Malinowsky, M., Shoham, O., Brill, J.P. 1989. An analysis of oil/water flow phenomena in horizontal pipes. SPE Paper 18836, pp. 155–167.

Baker, O., 1954. Simultaneous flow of oil and gas. Oil Gas J. 53, 184–195.

Bannwart, A.C., Rodriguez, O.M.H., de Carvalho, C.H.M., Wang, I.S., Vara, R.M.O., 2004. Flow patterns in heavy crude oil–water flow. J. Energy Resources Techno. Trans. Asme 126, 184–189.

Barnea, D., Luninski, Y., Taitel, Y., 1983. Flow pattern in horizontal and vertical 2 phase flow in small diameter pipes. Can. J. Chem. Eng. 61, 617–620.

Beretta, A., Ferrari, P., Galbiati, L., Andreini, P.A., 1997. Horizontal oil–water flow in small diameter tubes, flow patterns. Int. Commun. Heat Mass Transfer 24, 223–229.

Charles, M., Govier, G., Hodgson, G., 1961. The horizontal pipeline flow of equal density oil–water mixtures. Can. J. Chem. Eng. (February), 27–36.

Hapanowicz, J., Troniewski, L., 2002. Two-phase flow of liquid–liquid mixture in the range of the water droplet pattern. Chem. Eng. Process. 41, 165–172.

Hasson, D., Mann, U., Nir, A., 1970. Annular flow of 2 immiscible liquids. 1. Mechanisms. Can. J. Chem. Eng. 48, 514–520.

Liu, W.H., Guo, L.J., Wu, T.J., Zhang, X.M., 2003. An experimental study on the flow characteristics of oil–water two-phase flow in horizontal straight pipes. Chinese J. Chem. Eng. 11, 491–496.

Mandhane, J.M., Gregory, G.A., Aziz, K., 1974. A flow pattern map for gas–liquid flow in horizontal pipes. Int. J. Multiphase Flow 1, 537–553.

Nadler, M., Mewes, D., 1997. Flow induced emulsification in the flow of two immiscible liquids in horizontal pipes. Int. J. Multiphase Flow 23, 55–68.

Simmons, M.J.H., Azzopardi, B.J., 2001. Drop size distributions in dispersed liquid–liquid pipe flow. Int. J. Multiphase Flow 27, 843–859.

Sotgia, G., Tartarini, P., 2004. The flow of oil–water mixtures in horizontal pipes, state of the art and recent developments on pressure drop reductions and flow regime transitions. In 3rd International Symposium on Two-Phase Flow Modelling and Experimentation, Pisa.

Stahl, P., 2002. Rohrreaktor fuer Fluessigkeits-Reaktionen mit Gasbildung, volume Diss ETH Nr. 14507. Federal Institute of Technology, Zurich (Switzerland). Available from: <http://e-collection.ethbib.ethz.ch/cgi-bin/show.pl?type=diss&nr=14507>.

Trallero, J.L., Sarica, C., Brill, J.P., 1997. A study of oil/water flow patterns in horizontal pipes. Spe Production and Facilities 12, 165–172.

Wagner, W., Kruse, A. (Eds.), 1998. Properties of Water and Steam. Springer, Berlin.

Ward, J.P., Knudsen, J.G., 1967. Turbulent flow of unstable liquid–liquid dispersions – drop sizes and velocity distributions. Aiche J. 13, 356–365.

Wong, T.N., Yau, Y.K., 1997. Flow patterns in two-phase air–water flow. Int. Commun. Heat Mass Transfer 24, 111–118.

Yang, L., Azzopardi, B.J., Baker, G., Belzhagi, A., Giddings, D., 2004. The approach to stratification of a dispersed liquid–liquid flow at a sudden expansion. In 3rd International Symposium on Two-Phase Flow Modelling and Experimentation, Pisa.